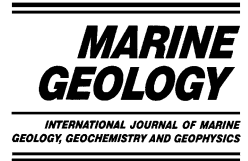




ELSEVIER

Marine Geology 190 (2002) 151–164



www.elsevier.com/locate/margeo

Aspects of carbon isotope biogeochemistry of late Quaternary sediments from the Marmara Sea and Black Sea

T. Abrajano^{a,*}, A.E. Aksu^b, R.N. Hiscott^b, P.J. Mudie^c

^a Department of Earth and Environmental Sciences, Rensselaer Polytechnic Institute, Troy, NY 12180, USA

^b Department of Earth Sciences, Centre for Earth Resources Research, Memorial University of Newfoundland, St. John's, NF, Canada A1B 3X5

^c Geological Survey of Canada-Atlantic, Bedford Institute of Oceanography, 1 Challenger Drive, Dartmouth, NS, Canada B2Y 4A2

Received 29 April 2001; accepted 19 February 2002

Abstract

The Marmara Sea is situated between the world's largest permanently anoxic basin, the Black Sea, and an enclosed marginal sea, the Aegean Sea, which experienced quasi-periodic sapropel deposition since Miocene time. It is connected to the Black Sea and the Aegean Sea through the Straits of Bosphorus and Dardanelles, respectively. Sapropel M1, which contains from 1 to 2% total organic carbon, was deposited in the Marmara Sea between 6 and 10.5 ka. We inferred the carbon isotopic composition of dissolved inorganic carbon (DIC) in the water column of the Marmara Sea before, during and after the deposition of sapropel M1 from the carbon isotopic composition of a planktonic foraminifera (*Turborotalita quinqueloba*) and individual hexadecanoic and octadecanoic fatty acids. The period of sapropel deposition is marked by a depletion of ¹³C in the water column DIC, contrary to what may be expected if sapropel deposition represents a period of enhanced primary productivity. Instead, we propose that both the relative ¹³C depletion of DIC during sapropel deposition and the absolute values we estimated ($\delta^{13}\text{C} = -13$ to -14‰) are consistent with enhancement of the relative contribution of ¹³C-depleted respired carbon to the water column DIC pool. Such enhancement possibly resulted from density stratification that existed during sapropel M1 deposition. The existence of density stratification is also argued from palynological and other lines of evidence (other papers in this issue), and is believed to have resulted from the encroachment of Black Sea water into the Sea of Marmara before 10 000 yr ago. Thus, sapropel M1 appears to have formed during periods of enhanced runoff and preservation and not enhanced primary productivity.

© 2002 Elsevier Science B.V. All rights reserved.

Keywords: Marmara Sea Gateway; Black Sea; sapropel; stable isotopes; compound-specific; isotope analysis; fatty acids; biogeochemistry; surface water salinity

1. Introduction

The Marmara Sea is situated between the

world's largest permanently anoxic basin, Black Sea, and an enclosed marginal sea, the Aegean Sea (NE extension of eastern Mediterranean Sea), which experienced quasi-periodic sapropel deposition since Miocene time (Fig. 1). It is connected to the Black Sea and the Aegean Sea through the Straits of Bosphorus and Darda-

* Corresponding author.

E-mail address: abrajt@rpi.edu (T. Abrajano).

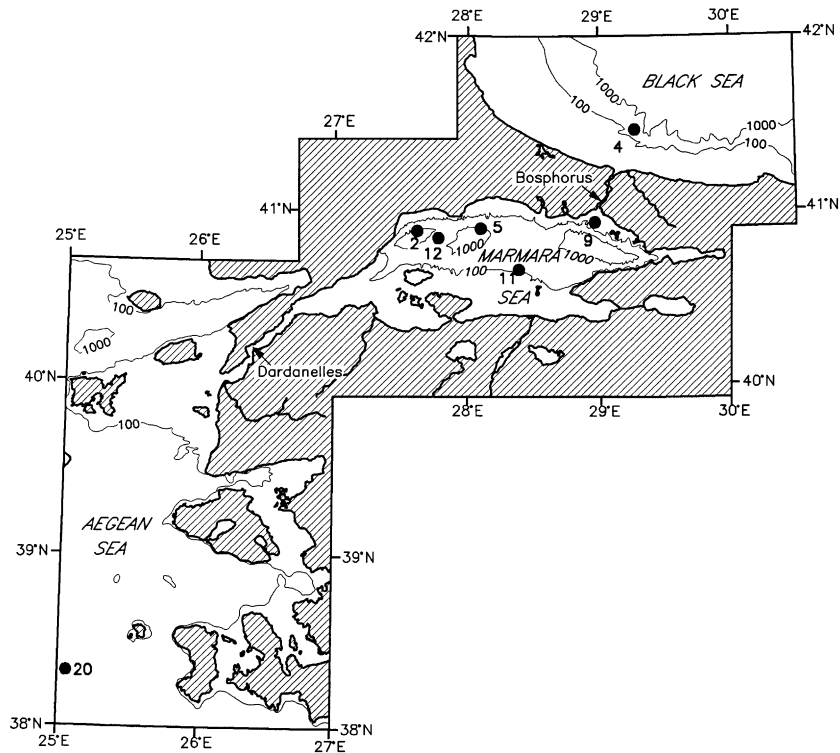


Fig. 1. Marmara Sea Gateway, showing the locations of the short gravity cores referred to in this study. 2=MAR97-02, 4=MAR98-04, 5=MAR94-05, 9=MAR98-09, 11=MAR97-11, 12=MAR98-12 and 20=Aegean Sea Core 20. Isobaths (100 and 1000) are in meters.

nelles, respectively. Our broad research objectives are: (1) to determine the role of the Marmara Sea Gateway in paleoceanographic evolution of the eastern Mediterranean and Black Seas, in particular the development of quasi-periodic sapropel in these regions, using micropaleontological, bulk isotopic and geochemical data in cores; (2) to determine the relative importance of sea-level changes, sediment supply and local tectonics in controlling the distribution of marine/lacustrine sedimentary deposits in a small, land-locked basin (the Marmara Sea) using sedimentological data and radiocarbon dates in cores; and (3) to establish the shallow crustal structural framework, with particular emphasis on determining the loci of Plio–Pleistocene deformation by mapping lineaments and faults using high-resolution seismic profiling. Several papers in this issue discuss other facets of this collaborative research. The present paper focuses on carbon isotopic variations ob-

served during sapropel deposition and the constraints these observations provide in reconstructing paleo-environments and organic matter sources for the deposition of sapropel M1. Carbon isotope data on bulk organic matter, fatty acids and carbonates are used along with palynological, paleontological and other geochemical observations to examine the conditions that led to the initiation and termination of sapropel deposition.

Increased organic matter concentrations during deposition of sapropel deposits in the Mediterranean region have been variously ascribed to basin-wide stagnation and subsequent basin anoxia (e.g. Vergnaud-Grazzini et al., 1977; Kidd et al., 1978) or enhanced planktonic productivity in surface waters ($> 500 \text{ g cm}^{-2} \text{ yr}^{-1}$) (Calvert, 1983; Calvert and Pedersen, 1993). The anoxia theory has spawned several working hypotheses: (i) periodic stratification and stagnation as the result of

large freshwater and glacial meltwater influxes entering the eastern Mediterranean from the Adriatic Sea and the Black Sea via the Aegean Sea (Tang and Stott, 1993); (ii) density stratification caused by freshwater influxes during changes from strongly arid to pluvial conditions in the eastern Mediterranean at the transitions from full to late glacial periods (Fairbridge, 1972); and (iii) stratification caused by heavy Nile floods at times of increased monsoonal precipitation over tropical eastern Africa (Rossignol-Strick, 1985). In earlier studies from the Aegean Sea, Aksu et al. (1995a,b) found little evidence for a major increase in primary productivity during the development of sapropel S1, and showed that sapropel S1 was deposited during a period of intense reduction in surface water salinities, with the Black Sea being the potential source for the fresher surface water through the Marmara Sea Gateway. More recently, fatty acid, *n*-alkane and dinoflagellate cyst data from a single core from the Aegean Sea (Core 20) were used to show that the onset of S1 deposition was marked by a decline in net primary productivity (NPP), which then increased notably during the later stages of deposition of S1 (Aksu et al., 1999). The decline in NPP was suggested by $\delta^{13}\text{C}$ variations in *n*-hexadecanoic fatty acids and *n*-octadecanoic fatty acids, both being interpreted as indicators of substrate $\delta^{13}\text{C}$ (i.e. dissolved inorganic carbon, DIC) composition. In contrast, total organic carbon (TOC) $\delta^{13}\text{C}$ measurements showed depletion of ^{13}C , which we interpreted to reflect enhanced terrestrial organic matter contribution to the total organic pool. This interpretation was further supported by increased deposition of terrestrial pollen and spores. Interestingly, subsequent measurement of $\delta^{13}\text{C}$ in *Globigerinoides ruber* independently confirmed our hypothesis that the compound-specific $\delta^{13}\text{C}$ patterns in Core 20 reflect a shift in DIC substrate $\delta^{13}\text{C}$, with S1 deposition representing an episode of basin-wide depletion of ^{13}C in DIC. This observation seriously contradicts any suggestion that the increased organic flux was caused by enhanced NPP. This paper examines similar processes that controlled sapropel deposition in the Marmara Sea, and compares isotopic observations in the

Marmara Sea to those made in the Aegean and Black Seas.

2. Data acquisition and methods

During the MAR94, MAR97, MAR98 and MAR00 cruises of the RV *Koca Piri Reis* of the Institute of Marine Sciences and Technology, respectively in 1994, 1997, 1998 and 2000, 65 ~2.5-m-long gravity cores were collected from the northeastern Aegean Sea, southwestern Black Sea and the Marmara Sea, using a 4-m-long corer with 10-cm internal diameter and 400 kg weight (Fig. 1). The core sites were carefully selected using ~7500 line-km of high-resolution boomer profiles, located by satellite navigation (GPS). Cores were stored upright onboard ship and were shipped to Memorial University of Newfoundland (MUN), where they were split, described and photographed. Sediment color was determined using the 'Rock-Color Chart' published by the Geological Society of America in 1984. Six key cores were identified, in which critical stratigraphic horizons determined in seismic profiles could be studied and dated. These cores were systematically sub-sampled for organic geochemical and stable isotopic studies. Approximately 20 cc of sediment was removed at 10-cm intervals from each core.

The amount of TOC and its carbon isotopic composition were determined in each sample at MUN. Samples were acidified using 30% HCl, and carbonate-free residues were dried overnight in an oven at 40°C. A small amount of sample (~15 mg) was transferred into 4×6-mm-thin capsules which were then sealed for elemental analysis using a Carlo-Erba NA 1500 Elemental Analyzer coupled to a Finnigan Mat 252 isotope-ratio mass spectrometer (IRMS). TOC was converted to CO₂, H₂O and other oxidized gases in the oxidation chamber and then passed through a reduction reagent (to remove excess O₂), a Mg(ClO₄)₂ water trap and a 1.2-m Poropak QS 50/80 chromatographic column at 70°C for final isolation. TOC quantification from measurement of generated CO₂ was accomplished using an external standard (sulfanilamide, C₆H₈N₂O₂S) and

a thermal conductivity detector (TCD). From the TCD, the CO₂ was carried by He to a ConFloII interface, which allows a portion of the He and combustion gases to enter directly the ion source of the IRMS for carbon isotopic measurement. The TOC concentration in the samples is back-calculated as weight percentage of dry weight sediment. All isotopic analyses are reported in standard δ notation referenced to PDB.

Pure fatty acid isotopic standards and BF₃-methanol for derivatization were acquired from Supelco, Inc. (Bellefonte, PA, USA). Fatty acid methyl esters of each compound were formed by reaction of free acids with BF₃-methanol at 100°C. Sediment samples were first dried, weighed and then saponified with 6 N KOH. The non-saponifiable fraction was separated from the saponifiable fraction by repeated extraction with methylene chloride. The basic aqueous solution was acidified with concentrated HCl to pH 1 and the fatty acids were separated by repeated extraction with methylene chloride. The separated fatty acids were esterified in the same way as pure standards.

Compound-specific $\delta^{13}\text{C}$ values for individual fatty acids were determined at the Isotope Biogeochemistry and Hydrology Laboratory, Rensselaer Polytechnic Institute, following procedures described previously (Abrajano et al., 1994; Aksu et al., 1999). Gas chromatographic (GC) temperature programs and acquisition parameters were as follows: 50°C to 150°C at 50°C min⁻¹; 150°C to 280°C at 10°C min⁻¹ with total run time of 30 min per sample. A 60-m DB5 MS 0.25-mm (ID) 0.25- μm film thickness capillary column was used, with a He carrier gas at a head pressure of 12.5 psi. GC injectors were set at 80°C to 280°C at 200°C min⁻¹. The GC/IRMS combustion interface and furnace temperatures were set at 300°C and 850°C, respectively.

The percent biogenic opal was determined by a single 5-h extraction of silica into a 2 M Na₂CO₃ solution at 85°C (Mortlock and Froelich, 1989). Dissolved silica in the solutions was determined by modified molybdate blue spectrophotometry at MUN. Quadruplicate analyses showed that the reproducibility of this technique was better than 0.4% biogenic SiO₂. Standard methods were

used for extraction of pollen, spores and dinoflagellate cysts, as described elsewhere in this volume (Mudie et al., 2002a,b).

3. Results and interpretation

3.1. Sedimentary data and chronology

Four allostratigraphic units (allounits) are identified in the late Quaternary successions of the Marmara Sea and Black Sea (Hiscott and Aksu, 2002). Allounit A extends from the seafloor downward to a \sim 12-ka (thousands of years before present) sequence boundary, which is an unconformity in water depths less than \sim 100 m and a correlative conformity in deeper area. In some cores from the Marmara Sea, Unit A is divided into two subunits: A1 (\sim 0–6 ka) and A2 (\sim 6–11 ka; Hiscott and Aksu, 2002). Allounit B is only present at water depths greater than \sim 90 m, and represents basinal or prodeltaic deposition during the 23–12-ka lowstand. Allounit C is a laminated sapropel (M2) with an age of \sim 23.5–29.5 ka. Cored sediments older than \sim 30 ka are not divided into allostratigraphic units because we have rarely cored these deposits, and have not dated any unconformities beneath the \sim 12-ka sequence boundary.

Two allounits are identified in the Quaternary succession in Black Sea. Allounit A extends from the seafloor a \sim 11-ka sequence boundary which represents the major shelf-crossing unconformity, α (Aksu et al., 2002a,b). Allounit B is only present along the shelf edge in water depths greater than 90 m, and represents deltaic deposition during the last glacial maximum; it has not been cored. Sediments below the major shelf-crossing unconformity are older than 30 ka and represent a diverse group of older Cenozoic deposits.

Thirty-nine shells extracted from several levels in 17 cores were radiocarbon-dated at the Isotrace Radiocarbon Laboratory of the University of Toronto and the Beta Analytical Laboratories, FL, USA (Aksu et al., 2002a). The chronostratigraphic framework for the Marmara Sea Gateway is established using \sim 7500 line-km of high-resolution seismic reflection profiles together cali-

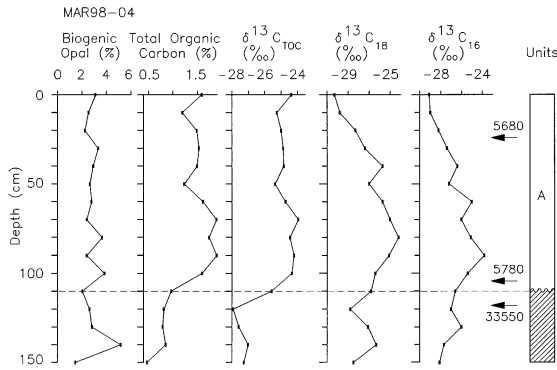


Fig. 2. Biogenic opal, TOC, $\delta^{13}\text{C}$ of TOC, and $\delta^{13}\text{C}$ of saturated fatty acids *n*-hexadecanoic acid (C16) and *n*-octadecanoic acid (C18) in Black Sea core MAR98-04. Allostratigraphic units A–C discussed in text. Location in Fig. 1.

brated by the radiocarbon ages (e.g. Aksu et al., 2002b; Hiscott et al., 2002).

3.2. TOC and carbon isotope composition

TOC values measured for the Marmara cores are shown in Figs. 2–6. In the Black Sea core MAR98-04, TOC values fluctuate between 1.6 and 2.0% throughout Allunit A, but show a sharp decline at the shelf-crossing major unconformity (Aksu et al., 2002b) from > 1.5% to 0.9% (Fig. 2). Measured TOC values are moderate to high in Unit A, ranging from 0.9 to 2.0% in basal Marmara Sea cores MAR97-02 and MAR98-12 and from 1.0 to 1.5% in the shelf cores

MAR97-11 and MAR98-09 (Figs. 3–6). Allunits A2 and C contain high concentrations of TOC in the basal cores MAR98-12 and MAR94-05, respectively, where TOC values are generally above 2.0%, locally exceeding 2.9%. TOC values are consistently low in Allunit B, ranging from 0.3 to 1.5% (Figs. 3–6).

‘Sapropel’ is defined as a discrete bed, > 1 cm thick, which contains greater than 2.0% TOC by weight, whereas a ‘sapropelic layer’ is defined to contain between 0.5 and 2.0% TOC by weight (Kidd et al., 1978). Therefore, all sediments recovered from the Marmara Sea as well as Allunit A in the Black Sea can be classified as sapropel deposits; however, Allunits A2 and C in the basal Marmara Sea cores MAR98-12 and MAR94-05, respectively, represent sapropel layers (discussed later). There are numerous discrete sapropel deposits in the Quaternary sediments of the eastern Mediterranean Sea, including the Aegean Sea. These deposits are labeled from the youngest to the oldest as S1, S2, S3 etc. (Vergnaud-Grazzini et al., 1977; Rossignol-Strick, 1985). To avoid confusion with these other deposits, the sapropel layers in the Marmara Sea are labeled as M1 and M2.

In the Black Sea core MAR98-04, the carbon isotopic composition of the TOC, $\delta^{13}\text{C}_{\text{TOC}}$, ranges from –24.0 to –25.4‰ in Allunit A (Fig. 2), most of which represents deposition during the middle Holocene (5780–5680 yr BP). These carbon isotopic values are slightly lighter than the

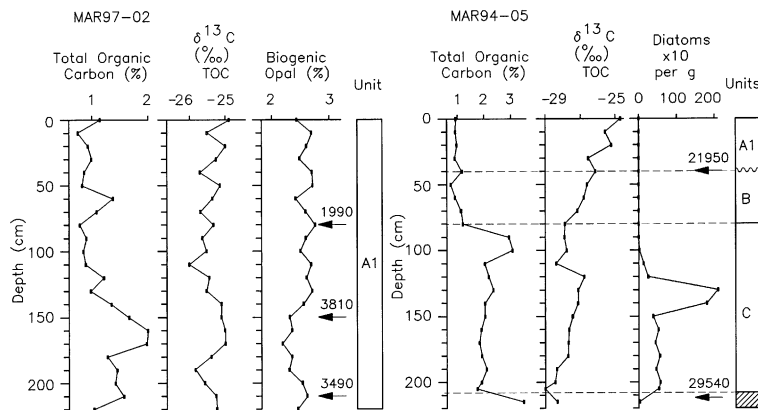


Fig. 3. TOC, $\delta^{13}\text{C}$ of TOC, and biogenic opal or diatom concentrations in Marmara Sea core MAR97-02 (left) and MAR94-05 (right). Allostratigraphic units A1, B, C discussed in text. Location in Fig. 1.

modern planktonic $\delta^{13}\text{C}$ values of -22‰ reported for the Black Sea (Deuser, 1970), and probably represent mixing of marine and terrestrial sources. The downcore transition from basal Allounit A to older sediments below the α unconformity is marked by a notable depletion of $\sim 4.0\text{‰}$ in the $\delta^{13}\text{C}_{\text{TOC}}$ values, with the carbon isotopic composition remaining relatively constant at -27.5‰ to the base of the core (Fig. 2). This major downcore depletion in the carbon isotopes reflects a radical shift in the source of the TOC from a predominantly terrestrial source in sediments below the unconformity to a marine source in Allounit A (Deines, 1980).

In the Marmara Sea cores, the $\delta^{13}\text{C}_{\text{TOC}}$ values in Allounit A are fairly constant at -24.5 to -25.0‰ (Figs. 3–6). In core MAR98-09, the downcore transition from Allo-subunits A1 to A2 is marked by a $\sim 2.0\text{‰}$ depletion in the carbon isotopic composition of the TOC (Fig. 6). In this core, the $\delta^{13}\text{C}_{\text{TOC}}$ values in Allo-subunit A2 remain remarkably constant at -26.6 to -26.8‰ , but show a $> 1.5\text{‰}$ enrichment at $\sim 110\text{-cm}$ depth in the core (Fig. 6). In core MAR98-12, the $\delta^{13}\text{C}_{\text{TOC}}$ values show a minor depletion downcore across Allo-subunit A1, with the A1–A2 transition defined by a small step-like depletion (Fig. 4). The carbon isotopic composition of Allounit 2 (sapropel M1) is -26.0‰ at the base of the unit, but exhibits a progressive enrichment to -25.3‰ at the transition to Allo-subunit A1 (Fig. 4). The $\delta^{13}\text{C}_{\text{TOC}}$ values in Allounit B are relatively constant at -25.5 to -26.0‰ (Fig. 4).

The southern Marmara shelf core MAR97-11 displays carbon isotopic stratigraphy similar to core MAR98-12; however, the transition from a predominantly marine isotopic signature of -24.2‰ to a predominantly terrestrial isotopic signature occurs in mid-Allounit A, with the $\delta^{13}\text{C}_{\text{TOC}}$ values in Allounit B remaining relatively constant at -25.5 to -26.0‰ (Fig. 5). The $\delta^{13}\text{C}_{\text{TOC}}$ composition of Allounit C (sapropel M2) in core MAR94-05 shows two distinct enrichment trends: at the base of Allounit C the carbon isotopic composition of the TOC is -29.0‰ (Fig. 3), but shows a progressive enrichment to -27.0‰ in mid-Allounit C, thereafter

shows a sharp decline to -28.8‰ , then a sustained enrichment upcore into Allounits B and A, with the $\delta^{13}\text{C}_{\text{TOC}}$ values reaching $\sim -25.0\text{‰}$ near the top of Allounit A (Fig. 3).

Compound-specific carbon isotope analyses of the dominant saturated fatty acids (*n*-hexadecanoic C16 and *n*-octadecanoic C18) are shown in Figs. 2 and 4–6. In core MAR98-12, the highest concentrations of TOC occur above the intervals with the most depleted $\delta^{13}\text{C}$ concentrations in both hexadecanoic and octadecanoic fatty acids in Allo-subunit A2 (Fig. 4). This relationship is similar to data for Core 20 from the Aegean Sea (Aksu et al., 1999). As in the Aegean samples, there are some stratigraphic disparities between the $\delta^{13}\text{C}$ values measured for C16 and C18, but the broader temporal features of the isotopic patterns are quite similar. For the Aegean deposits, we likewise observed that the temporal trends in $\delta^{13}\text{C}$ values of the TOC and the fatty acids showed no simple concordance, with clear disparities before and after sapropel S1 deposition. Nevertheless, a shift to $\delta^{13}\text{C}$ depletion from the bottom to the top of the sapropel S1 was apparent in both the compound-specific and bulk TOC data. In core MAR98-12, some degree of concordance between the bulk and fatty acid $\delta^{13}\text{C}$ values was again observed. A decline in $\delta^{13}\text{C}$ values at the onset of sapropel deposition, a minimum between 100 and 130 cm and a steady rise to $\delta^{13}\text{C}$ enriched values towards the top of the sapropel deposit. In Allo-subunits A1 and B, a higher degree of discordance between the bulk and fatty acid $\delta^{13}\text{C}$ values is apparent. Nevertheless, the $\delta^{13}\text{C}$ values for hexadecanoic acid appear to show temporal correspondence with the bulk TOC $\delta^{13}\text{C}$ values.

The $\delta^{13}\text{C}$ values observed for C16 and C18 fatty acids in the shallower core MAR97-11 show a very gradual depletion of $\delta^{13}\text{C}$ throughout Allounit B, a pattern also noted for the bulk $\delta^{13}\text{C}$ values (Fig. 5). However, in Allounit A concordant $\delta^{13}\text{C}$ fluctuation was observed in C16 and C18, with bulk $\delta^{13}\text{C}$ values showing only a monotonic increase. It is noteworthy that Allounit A in core MAR97-11 temporally corresponds to the deposition of organic-rich Allounit A2 in core MAR98-12. The most $\delta^{13}\text{C}$ -depleted values for

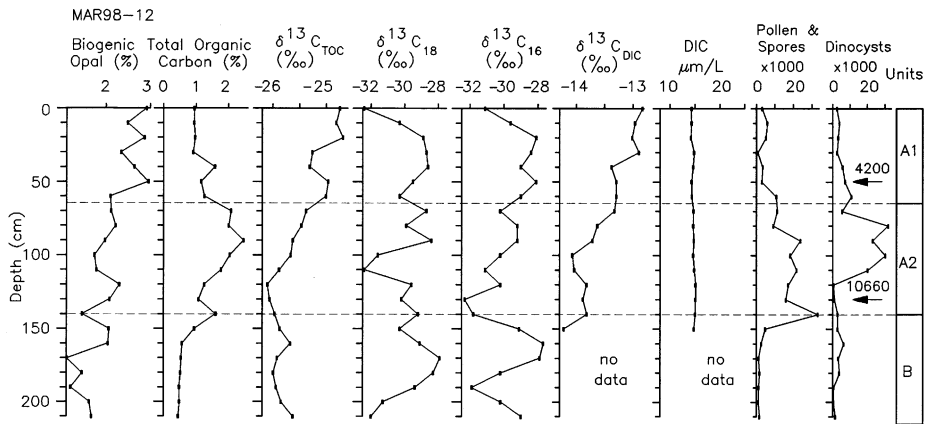


Fig. 4. Biogenic opal, TOC, $\delta^{13}C$ of TOC, $\delta^{13}C$ of saturated fatty acids *n*-hexadecanoic acid (C16) and *n*-octadecanoic acid (C18), and calculated $\delta^{13}C$ of DIC and DIC concentrations in Marmara Sea core MAR98-12. Allostratigraphic units A1, A2, B discussed in text. Location in Fig. 1.

C16 and C18 are similar at about -32‰ for these time-equivalent units.

Core MAR98-09 was collected from the Marmara Sea shelf immediately adjacent to the Strait of Bosphorus. The stratigraphic correlation between TOC levels and compound-specific and bulk TOC $\delta^{13}C$ values is again clearly displayed (Fig. 6). The high TOC levels were observed in Allo-subunits A1 and the lower portion of A2, which also exhibits the lowest $\delta^{13}C$ values for

bulk and individual fatty acids. The lowest $\delta^{13}C$ values approach the same levels as in sapropel deposits in core MAR98-12. In contrast to observations made in cores MAR98-12 and MAR97-11, a good temporal correspondence between bulk and compound-specific $\delta^{13}C$ values is evident in core MAR98-09 (Fig. 6). The onset of greater TOC deposition corresponded to an immediate decline in $\delta^{13}C$ values for TOC and hexadecanoic acid. The corresponding decline in $\delta^{13}C$ values for

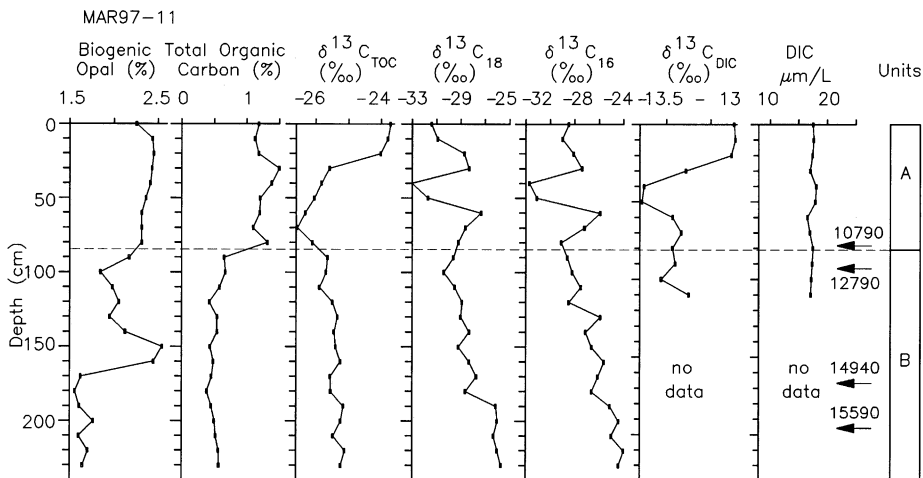


Fig. 5. Biogenic opal, TOC, $\delta^{13}C$ of TOC, $\delta^{13}C$ of saturated fatty acids *n*-hexadecanoic acid (C16) and *n*-octadecanoic acid (C18), and calculated $\delta^{13}C$ of DIC and DIC concentrations in Marmara Sea core MAR97-11. Allostratigraphic units A, B discussed in text. Location in Fig. 1.

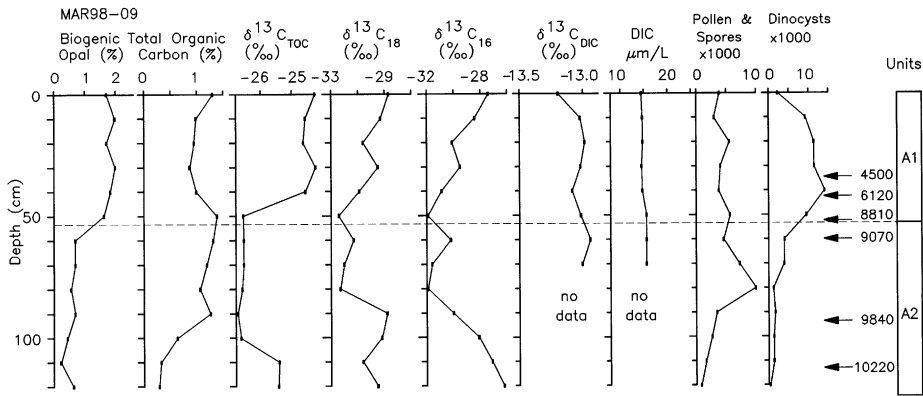


Fig. 6. Biogenic opal, TOC, $\delta^{13}\text{C}$ of TOC, $\delta^{13}\text{C}$ of saturated fatty acids *n*-hexadecanoic acid (C16) and *n*-octadecanoic acid (C18), and calculated $\delta^{13}\text{C}$ of DIC and DIC concentrations in Marmara Sea core MAR98-09. Allostratigraphic units A1, A2 discussed in text. Location in Fig. 1.

C18 fatty acids is delayed slightly, although the temporal correspondence of all three $\delta^{13}\text{C}$ values for the rest of the core is quite apparent.

The Black Sea core MAR98-04 shows distinctly different isotopic patterns to those measured in cores from the Marmara Sea (Fig. 2). The most outstanding difference in core MAR98-04 compared to these other cores is the reverse relationship between TOC and bulk and fatty acid $\delta^{13}\text{C}$ values. The highest TOC levels in core MAR98-04 are in the lower portion of Allounit A. The onset of increased TOC deposition in this unit is clearly marked by a shift to enriched $\delta^{13}\text{C}$ values for bulk and fatty acids, opposite to that observed for cores from the Marmara Sea. Furthermore, a very good correspondence in $\delta^{13}\text{C}$ values between bulk TOC and C16 and C18 fatty acids is quite evident, especially for deposition above the major shelf-crossing unconformity α (Fig. 2). The onset of deposition of Allounit A is marked by an increase in $\delta^{13}\text{C}$ values, followed by a decrease of TOC at mid-Allounit A. This variation is again opposite to that observed for the Marmara Sea and even the Aegean Sea Core 20 studied by Aksu et al. (1999). The reason for this difference is most likely related to the very high sedimentation rate of Allounit A in core MAR98-04: pollen+spore and dinoflagellate cyst assemblages are essentially the same as those in the mid-Holocene pre-colonization (~ 4 ka) period of the Marmara Sea cores (Mudie et al., 2002a,b).

3.3. Biogenic opal

Biogenic opal concentrations in Black Sea core MAR98-04 show little variation across Allounit A, oscillating between 2 and 4% (Fig. 2). These opaline silica values reflect the relatively high biogenic productivity in the Black Sea (Schrader, 1978).

Biogenic opal concentrations show much greater variability in the Marmara Sea cores (Figs. 3–6). In core MAR98-09, immediately south of the Strait of Bosphorus, the biogenic opal values range between 1.6 and 2.0% in Allo-subunit A1, but decrease to $< 1.0\%$ in Allo-subunit A2, and remain consistently low (0.2–0.9%) across Allo-subunit A2. Sedimentation rate is much higher in Subunit A2 than in A1 (Fig. 6). In the basal cores MAR97-02 and MAR98-12, biogenic opal concentrations are relatively high in Allo-subunit A1, ranging from 2.3 to 3.0% (Figs. 3 and 4). In core MAR98-12 biogenic opal values are notably lower in Allo-subunits A2 (1.4–2.1%) and B (0.1–0.5%). In the southern shelf core MAR97-11, biogenic opal concentrations range between 2.2 and 2.4% across Allounit A and the upper portion of Allounit B, but decrease to 1.5–1.7% in the lower portion of Allounit B (Fig. 5). In cores MAR97-02, MAR98-09 and MAR98-12, the biogenic opal distributions show a nearly reciprocal relationship with the TOC abundances (Figs. 3, 4 and 6). Biogenic opal was not measured in core MAR94-05;

however, an inventory of diatoms in the silt-size fraction shows that Allounits A and B are barren of diatoms but Allounit C contains common freshwater dinoflagellates (Mudie et al., 2001) and variable quantities of diatoms (Fig. 3).

In general, most siliceous tests are produced by diatoms, silicoflagellates, radiolarians and to a lesser extent siliceous sponges. Because of the high degree of undersaturation of silica in the oceans, the skeletal elements of these microfossils are rapidly destroyed following organic decomposition (Broecker and Peng, 1982). Most of the silica is recycled within the upper 100 m of the oceans. The rate of silica dissolution decreases greatly with increasing water depth. Preservation in sediments is controlled by the rate of production in surface waters, but also sedimentation rates, vertical temperature distribution and dissolved silica concentrations in the ocean waters (Hurd and Theyer, 1975). Despite extensive dissolution, biogenic opal is widely distributed in oceanic sediments, and the sedimentary abundance patterns of biogenic silica in surface sediments closely mimic patterns of biogenic opal productivity (Leinen et al., 1986). Therefore, biogenic opal concentrations in marine sediments may be used as a proxy for paleoproductivity in the oceans (e.g. Bohrmann and Stein, 1989).

4. Discussion

What does sapropel M1 deposition in the Marmara Sea represent? The patterns of organic abundance, bulk organic $\delta^{13}\text{C}$, compound-specific $\delta^{13}\text{C}$ and carbonate carbon $\delta^{13}\text{C}$ in the Marmara Sea cores are similar to patterns previously described for the Aegean Sea sapropel S1. These observations collectively indicate that the water column DIC was depleted in $\delta^{13}\text{C}$ during sapropel deposition, possibly due to extensive CO_2 recycling by organic matter respiration. An increased relative contribution of respired CO_2 is also compatible with the development of density stratification during the deposition of sapropel M1 in the Marmara Sea, as this condition will reduce atmospheric CO_2 participation and conversely enhance recycled CO_2 input (e.g. Freeman et al., 1994).

The following examines in detail the observations and processes that occurred during the onset and closure of enhanced organic matter deposition in sapropel M1.

In core MAR98-12, the onset of sapropel deposition (Allounit B–Subunit A2 transition) is marked by a decline in the $\delta^{13}\text{C}$ values for C16 and C18 fatty acids. Conversely, the transition out of sapropel deposition (Allo-subunit A2 to A1 transition) represents a period of increasing $\delta^{13}\text{C}$. Since hexadecanoic fatty acids are biosynthesized in relatively large amounts by all autotrophic algae (e.g. Schouten et al., 1998), we interpret the first order C16 $\delta^{13}\text{C}$ pattern to imply a change in $\delta^{13}\text{C}$ of the DIC substrate of photosynthetic fixation during the two aforementioned transitions. Specifically, sapropel deposition appears to be accompanied by a depletion of ^{13}C in the DIC substrate. If this interpretation is valid, the data contradict the notion that enhanced NPP triggered sapropel deposition.

Are there other constraints to our interpretation? We measured the $\delta^{13}\text{C}$ in planktonic foraminifera to enable calculation of DIC $\delta^{13}\text{C}$ at the time of formation. In particular, a planktonic foraminifera *Turborotalita quinqueloba* was observed throughout Allounits A2 and A1, but unfortunately not in Allounit B (see Aksu et al., 2002a). Measurement of carbonate $\delta^{13}\text{C}$ in *T. quinqueloba* reveals that compared to Allo-subunit A1, Allo-subunit A2 indeed represents a period of lowered $\delta^{13}\text{C}$ of DIC (Fig. 4). Thus, the increased compound-specific $\delta^{13}\text{C}$ values measured on the fatty acids towards the top of Allo-subunit A2 (sapropel M1) are consistent with a relative increase in $\delta^{13}\text{C}$ of DIC at the termination of sapropel deposition. It is notable that the $\delta^{13}\text{C}$ values calculated for DIC ranged from -12.8‰ to -14.1‰ , and are depleted in ^{13}C . We therefore suggest that respired CO_2 contribution was important during sapropel deposition in this case. Using the calculated values of $\delta^{13}\text{C}$ for DIC and the $\delta^{13}\text{C}$ values measured for the *n*-hexadecanoic acid, we can calculate the DIC concentrations in the water column from approximate formulations suggested by Freeman et al. (1994). For these calculations, we incorporated a 3.5‰ shift between TOC and $\delta^{13}\text{C}$ of hexadecanoic acid (cf. Freeman

et al., 1994; Schouten et al., 1998). Calculation of $\text{CO}_{2,\text{aq}}$ using the above relation yields a narrow range of 17.2–18.2 μM , which is within the range of expected values (8–25 μM) for surface ocean waters (Fig. 3). This restricted value of $\text{CO}_{2,\text{aq}}$ is also consistent with modern-day near-surface $\text{CO}_{2,\text{aq}}$ concentrations reported for the Black Sea of 17 μM (Freeman et al., 1994). If the $\text{CO}_{2,\text{aq}}$ concentrations were truly restricted to this range during the deposition of Allo-subunits A2 and A1, the enhanced deposition of organic matter in Allo-subunit A2 did not occur during a period of reduced $p\text{CO}_2$ (or enhanced NPP). It follows that the increasing fatty acid $\delta^{13}\text{C}$ values from the base of Allo-subunit A2 into Allo-subunit A1 cannot be reconciled with a decrease in NPP. Indeed, it is possible to attribute the increased ^{13}C in fatty acids in Allo-subunit A1 to enhanced autochthonous NPP in spite of the fact that the total TOC was decreasing at the same time. This interpretation is consistent with the overall increase in total planktonic foraminifera and biogenic opal from Allo-subunit A2 to A1. Hence, the bulk of organic matter found in Allo-subunit A2 must either be an enhanced allochthonous component derived from outside of the Marmara Sea or could represent enhanced preservation (see below).

Although the organic carbon isotopic record of Allounit B is not concordant with $\delta^{13}\text{C}$ measurements of its planktonic foraminifera, there is an interesting shift to $\delta^{13}\text{C}$ -enriched values just prior to deposition of Allo-subunit A2. This pattern was also observed in the Aegean Sea Core 20, and was interpreted to reflect a trend towards increasing NPP that was ‘interrupted’ by sapropel deposition (Aksu et al., 1999). In the Aegean sapropel, that suggestion was supported by palynological observations including the abundance of gonyaulacoid species (e.g. *Spiniferites*). Whereas Allounit B is largely devoid of planktonic foraminifera, we point to the high concentrations of benthic foraminifera in this unit (Kaminski et al., 2002) and the increase in biogenic opal concentrations near the top of Allounit B (Fig. 4) as supportive evidence for a possible increase in NPP prior to sapropel deposition. Dinoflagellate cyst concentrations in Allounit B are about the same

as in Allo-subunit A1 (Fig. 4) but the composition of the assemblage is very different. In Allounit B, autotrophic gonyaulacoid brackish-freshwater dinoflagellate cysts are common (mostly *Spiniferites cruciformis*) and heterotrophic species are rare. In contrast, Allo-subunit A1 is dominated by marine and euryhaline autotrophic cysts of *Gonyaulax* species (see Mudie et al., 2002b) and cysts of heterotrophic protoperidinioid species are also common. As in the Aegean Sea S1 sapropel, there is a peak of heterotrophic *Brigantedinium* cysts in the sapropel layer at the base of Allo-subunit A2 (sapropel M1). In the upper portion of M1, pollen–spore concentrations remain high but there is a shift to dominance of gonyaulacoid dinoflagellate species. These changes from oxidation-sensitive protoperidinioid species to more resistant gonyaulacoid species within the sapropel units of both the Aegean and Marmara Seas suggest that there is a sediment redox threshold value corresponding to TOC of ~ 1 above which dinoflagellate cysts and pollen–spore deposits are not susceptible to oxidative dissolution (cf. Zonneveld et al., 2001).

The carbon isotopic patterns observed in the prodelta deposits of core MAR97-11 corroborate the interpretation of MAR98-12. In MAR97-11, TOC barely exceeds 1%. The highest TOC levels were recorded in Allounit A. Corresponding fatty $\delta^{13}\text{C}$ values show a steady decline from the base to the top of Allounit B, but a notable increase prior to a sharp decrease from 40 to 50 cm. Although TOC concentrations do not qualify these deposits to be called ‘sapropel layers’, they nevertheless show the same pattern noted in MAR98-12. We surmise that this brief episode characterized by $\delta^{13}\text{C}$ -depleted fatty acids correlates with M1 sapropel deposition in core MAR98-12. In both cores MAR97-11 and, MAR98-12, the decline in compound-specific $\delta^{13}\text{C}$ is of the same magnitude (3–4‰), and in each case results in an estimated DIC concentration of 17–18 μM during and after the deposition of organic-rich layers. We interpret this broad consistency as indicative of a basin-wide process of increased contribution of respired CO_2 during the period of enhanced organic matter deposition and preservation. If there was enhancement of

organic matter input during the formation of the organic-rich layers, that contribution must have an allochthonous origin because enhanced NPP would have led to depletion of DIC concentrations and enrichment of ^{13}C in the organic deposits, neither of which was observed. Enhanced preservation beneath a stratified water column however, can easily be reconciled with an increased contribution of respired organic carbon into the water column DIC pool. It is also noteworthy that for core MAR97-11, the $\delta^{13}\text{C}$ values for the TOC are clearly depleted during the deposition of the organic-rich layers as seen in MAR98-12. Although this stratigraphic pattern is broadly consistent with the patterns of $\delta^{13}\text{C}$ observed in C16 and C18 fatty acids, the depletion in ^{13}C in TOC at the initiation of organic matter deposition appears to precede the decline in $\delta^{13}\text{C}$ values for the fatty acids. This observation can be explained by the proportionately greater contribution of ^{13}C -depleted terrestrial material in the shallower portions of the Marmara Sea. If this enhanced terrestrial contribution to the TOC pool represents greater riverine input from the surrounding watersheds or via the Black Sea, then density stratification promoting a greater contribution of a recycled organic component to the DIC pool would be expected to coincide with an increased terrestrial contribution. The striking correlation between $\delta^{13}\text{C}$ values for the fatty acids and the independently estimated $\delta^{13}\text{C}$ values of DIC is again worth noting, given their collective implication that the substrate DIC was depleted in ^{13}C during sapropel deposition.

The same broad isotopic patterns are likewise observed in core MAR98-09, where deposition of ^{13}C -depleted fatty acids again corresponds to the highest TOC levels in Allo-subunit A2. Similarly, there is a broad correspondence between $\delta^{13}\text{C}$ values for the fatty acids and TOC. The notable deviation from the patterns observed in cores MAR97-11 and MAR98-12 is the lack of variation in the calculated $\delta^{13}\text{C}$ values for DIC in MAR98-09. It is yet unclear why the DIC temporal carbon isotopic pattern observed in cores MAR98-12 and MAR97-11 was not observed in core MAR98-09. A key difference between core MAR98-09 and the other Marmara cores is its

location near the Strait of Bosphorus. We are continuing to evaluate additional cores from this location, but two possibilities that should be considered are the impact of carbon or nutrient input from the Black Sea and the nature of water circulation or stratification in the deltaic environments represented by MAR98-09.

The Black Sea core MAR98-04 offers a striking contrast to the observations presented above for the Marmara Sea. Normal marine deposition in this part of the Black Sea (Fig. 1) is only apparent after 6 ka, but initial Holocene contact between waters of the Black Sea and the Marmara Sea occurred at ~ 10 – 12 ka (Aksu et al., 2002a,b; Hiscott et al., 2002). Black Sea Alloumit A unconformably overlies older sediments which are interpreted to represent a lacustrine phase of deposition (Mudie et al., 2002a,b). TOC contents in excess of 1.5% were measured in the lower half of Alloumit A, along with the most ^{13}C -enriched TOC and C16 and C18 fatty acids. Such $\delta^{13}\text{C}$ patterns are consistent with organic matter deposition during periods of enhanced NPP (cf. Calvert and Pedersen, 1993), with increasing $\delta^{13}\text{C}$ possibly representing fixation under DIC-depleted conditions. Unfortunately, we were unable to derive $\delta^{13}\text{C}$ estimates for DIC in core MAR98-04 because of the absence of planktonic foraminifera. Nevertheless, the contrasting $\delta^{13}\text{C}$ pattern observed in MAR98-04 compared to the three Marmara Sea cores suggests a biogeochemical contrast between the two interconnected basins. The organic depositional period represented by the sapropel deposits in both basins overlapped, but the entire lower portion of Alloumit A in core MAR98-04 was deposited over a short time frame (~ 1000 yr) corresponding only to the very top of sapropel M1 in the Marmara Sea cores. Thus, the bulk of organic matter deposition described above for the Marmara Sea largely pre-dates the lower part of Alloumit A in the Black Sea core MAR98-04.

The reason for the contrast in organic carbon isotopic patterns in the Black Sea and Marmara Sea is not entirely resolved by our data, but we suggest that this resulted from the very different eutrophication status of the two depositional systems. In the nutrient-rich Black Sea, the availabil-

ity of the DIC substrate could have rate-limited the primary production. High primary production, corroborated by high biogenic opal concentrations, could draw down the DIC substrate concentration enough to lower the effective fractionation between fixed organic carbon and DIC (i.e. ϵ). Such dependence of organic $\delta^{13}\text{C}$ on DIC was indeed shown by Freeman et al. (1994) in the modern Black Sea. Furthermore, rapid photosynthetic utilization of ^{12}C also enriches the DIC pool in ^{13}C . In contrast, a lower rate of photosynthetic fixation in the relatively 'nutrient-poor' water column of the Marmara Sea (consistent with lower biogenic opal production) did not result in as much DIC drawdown. Under such conditions of biological fixation, the fractionation factor (ϵ) is maximized. This condition, combined with the formation of a low-salinity lid on the Marmara Sea from incursion of Black Sea water (Aksu et al., 2002a; Hiscott et al., 2002), led to the enhancement of respiration-derived DIC in the photic zone. Hence, the decrease in $\delta^{13}\text{C}$ values recorded by the fatty acids during sapropel deposition can be attributed to organic carbon recycling.

5. Conclusions

Carbon isotopic observations made on several sediment cores collected from the Marmara Sea and the Black Sea provide serious constraints on the paleo-environments and organic matter sources for the formation of sapropel M1. The $\delta^{13}\text{C}$ record from phytoplanktonic foraminifera and individual fatty acids independently suggest a measurable depletion in DIC ^{13}C in the water column during sapropel deposition, an isotopic shift that is inconsistent with enhanced NPP during sapropel formation. Enhanced NPP generally results in enrichment of ^{13}C because of reduced DIC concentrations resulting from DIC drawdown. We interpret the ^{13}C depletion in DIC to mean that more recycled CO_2 produced from organic decomposition was incorporated in the water column during sapropel deposition. This interpretation is consistent with the presence of water

stratification that limited atmospheric CO_2 input while enhancing the input of respired CO_2 . Such conditions could have been brought about by significant influx of freshwater into the Marmara Sea through the Bosphorus Strait. In contrast, enhanced organic matter deposition in the Black Sea core suggests ^{13}C enrichment during organic matter deposition, consistent with the drawdown effect on DIC of enhanced NPP. It is presently unclear why dramatic differences in sapropel depositional patterns are observed between the two adjacent depositional basins, but we propose that this arises from differences in their hydrodynamic and nutrient status at the time of sapropel formation.

Acknowledgements

We thank Prof. Dr. Erol Izdar, the Director of the Piri Reis Foundation for Maritime and Marine Resources Development and Education, and Prof. Dr. Orhan Uslu, the Director of the Institute of Marine Sciences and Technology, for their support and encouragement. We extend our special thanks to the officers and crew of the RV *Koca Piri Reis* for their assistance in data acquisition, in particular Captain Mehmet Özsaygılı and Chief Engineer Ömer Çubuk. We acknowledge the assistance of Michelle Alexander in opaline silica determinations, Alison Pye in TOC and bulk stable isotopic analyses, Linda Winsor and Carina Ramos in the compound-specific isotope measurements. We acknowledge start-up research funds and NSF support (BES-9871241) for T.A. at Rensselaer Polytechnic Institute, research funds from the Natural Sciences and Engineering Research Council of Canada (NSERC) to A.E.A. and R.N.H., ship-time funds from NSERC to A.E.A. and R.N.H., travel funds from the Dean of Science of Memorial University of Newfoundland, and a special grant from the Piri Reis Foundation for Maritime and Marine Resources Development and Education. Journal reviewers J. Silliman and J. Fang critically read the manuscript and provided many valuable comments and suggestions.

References

- Abrajano, T.A., Murphy, D.E., Fang, J., Comet, P., Brooks, J., MacDonald, I., 1994. $^{13}\text{C}/^{12}\text{C}$ ratios in fatty acids in marine mytilids with or without bacterial symbionts. *Org. Geochem.* 21, 611–617.
- Aksu, A.E., Yaşar, D., Mudie, P.J., 1995a. Paleoclimatic and paleoceanographic conditions leading to development of sapropel layer S1 in the Aegean Sea basins. *Palaeoclimatol. Palaeogeogr. Palaeoecol.* 116, 71–101.
- Aksu, A.E., Yaşar, D., Mudie, P.J., Gillespie, H., 1995b. Late glacial–Holocene paleoclimatic and paleoceanographic evolution of the Aegean Sea: micropaleontological and stable isotopic evidence. *Mar. Micropaleontol.* 25, 1–28.
- Aksu, A., Abrajano, T., Mudie, P.J., Yaşar, D., 1999. Organic geochemical and palynological evidence for terrigenous origin of the organic matter in Aegean Sea sapropel S1. *Mar. Geol.* 153, 303–318.
- Aksu, A.E., Hiscott, R.N., Kaminski, M.A., Mudie, P.J., Gillespie, H., Abrajano, T., Yaşar, D., 2002. Last glacial–Holocene paleoceanography of the Black Sea and Marmara Sea: stable isotopic, foraminiferal and coccolith evidence. *Mar. Geol.*, S0025-3227(02)00343-2.
- Aksu, A.E., Hiscott, R.N., Yaşar, D., İşler, F.I., Marsh, S., 2002. Seismic stratigraphy of Late Quaternary deposits from the southwestern Black Sea shelf: evidence for non-catastrophic variations in sea-level during the last 20000 years. *Mar. Geol.*, S0025-3229(02)00343-2.
- Bohrmann, R., Stein, R., 1989. Biogenic silica at ODP Site 647 in the southern Labrador Sea: occurrence, diagenesis, and paleoceanographic implications. In: Srivastava, S.P., Arthur, M., Clement, B. et al. *Proc. ODP Sci. Results* 105, 155–170.
- Broecker, W.S., Peng, T.H., 1982. *Tracers in the Sea*. Eldigio Press, Palisades, NY, 690 pp.
- Calvert, S.E., 1983. Geochemistry of Pleistocene sapropels and associated sediments from the eastern Mediterranean. *Oceanol. Acta* 6, 255–267.
- Calvert, S.E., Pedersen, T.F., 1993. Geochemistry of recent oxic and anoxic marine sediments: implication for the geological record. *Mar. Geol.* 113, 67–88.
- Deines, P., 1980. The isotopic composition of reduced carbon. In: Fritz, P., Fontes, J.C. (Eds.), *Handbook of Environmental Isotope Geochemistry*. Elsevier, Amsterdam, pp. 329–406.
- Deuser, W.G., 1970. Isotopic evidence for diminishing supply of available carbon during diatom bloom in the Black Sea. *Nature* 225, 169.
- Fairbridge, R.W., 1972. Quaternary sedimentation in the Mediterranean region controlled by tectonics, paleoclimates and sea level. In: Stanley, D.J. (Ed.), *The Mediterranean Sea*. Dowden, Hutchinson and Ross, Stoudsburg, PA, pp. 99–113.
- Freeman, K.H., Wakeham, S., Hayes, J., 1994. Predictive isotopic biogeochemistry: Hydrocarbons from anoxic marine basins. *Org. Geochem.* 21, 629–644.
- Hiscott, R.N., Aksu, A.E., 2002. Late Quaternary history of the Marmara Sea and Black Sea from high-resolution seismic and gravity-core studies. *Mar. Geol.*, S0025-3227(02)00350-x.
- Hiscott, R.N., Aksu, A.E., Yaşar, D., Kaminski, M.A., Mudie, P.J., Kostylev, V., MacDonald, J., İşler, F.I., Lord, A.R., 2002. Deltas south of the Bosphorus Strait record persistent Black Sea outflow to the Marmara Sea since ~10 ka. *Mar. Geol.*, S0025-3227(02)00344-4.
- Hurd, D.C., Theyer, F., 1975. Changes in the physical and chemical properties of biogenic silica from the central equatorial Pacific. *Adv. Chem. Ser.* 147, 211–230.
- Kaminski, M.A., Aksu, A.E., Box, M., Hiscott, R.N., Filipescu, S., Al-Salameen, M., 2002. Late glacial to Holocene benthic foraminifera in the Marmara Sea: implications for Black Sea–Mediterranean Sea connections following the last deglaciation. *Mar. Geol.*, S0025-3227(02)00347-x.
- Kidd, R.B., Cita, M.B., Ryan, W.B.F., 1978. Stratigraphy of eastern Mediterranean sapropel sequences recovered during DSDP Leg 42A and their paleoenvironmental significance. In: Hsü, K.J., Montadert, L. et al. (Eds.), *Initial Reports of the Deep Sea Drilling Project 42, part 1*. U.S. Government Printing Office, Washington, DC, pp. 421–443.
- Leinen, M., Heath, G.R., Biscay, P.E., Kolla, V., Thiede, J., 1986. Distribution of biogenic silica and quartz in recent deep sea sediments. *Geology* 14, 199–203.
- Mortlock, R.A., Froelich, P.N., 1989. A simple method for the rapid determination of biogenic opal in pelagic marine sediments. *Deep-Sea Res.* 36, 1415–1426.
- Mudie, P.J., Aksu, A.E., Yaşar, D., 2001. Late Quaternary dinoflagellate cysts from the Black, Marmara and Aegean seas: variations in assemblages, morphology and paleosalinity. *Mar. Micropaleontol.* 43, 155–178.
- Mudie, P.J., Rochon, A., Aksu, A.E., 2002. Pollen Stratigraphy of Late Quaternary cores from Marmara Sea: land-sea correlation and carbon sources in sapropel layers. *Mar. Geol.*, S0025-3227(02)00349-3.
- Mudie, P.J., Rochon, A., Aksu, A.E., Gillespie, H., 2002. Dinoflagellate cysts and freshwater alga and fungal spores as salinity indicators in Late Quaternary cores from Marmara and Black Seas. *Mar. Geol.*, S0025-3227(02)00348-1.
- Rosignol-Strick, M., 1985. Mediterranean Quaternary sapropels, an immediate response of the African monsoon to variation of insolation. *Palaeogeogr. Palaeoclimatol. Palaeoecol.* 49, 237–263.
- Schouten, S., Klein Breteler, W., Blokker, P., Schogt, N., Ruppstra, W., Grice, K., Baas, M., Sinnighe Dampste, J., 1998. Biosynthetic effects on the stable carbon isotope compositions of algal lipids: implications for deciphering the carbon isotopic biomarker record. *Geochim. Cosmochim. Acta* 62, 1397–1406.
- Schrader, H.-J., 1978. Quaternary through Neogene history of the Black Sea, deduced from the paleoecology of diatoms, silicoflagellates, ebridians and chrysomonads. In: Ross, D.A., Neprochnov, T.P. et al. (Eds.), *Initial Reports of the Deep Sea Drilling Project 42, part 2*. pp. 789–901.

- Tang, C.M., Stott, L.D., 1993. Seasonal salinity changes during Mediterranean sapropel deposition 9000 years B.P.: evidence from isotopic analyses of individual planktonic foraminifera. *Paleoceanography* 8, 473–493.
- Vergnaud-Grazzini, C., Ryan, W.B.F., Cita, M.B., 1977. Stable isotope fractionation, climate change and episodic stagnation in the eastern Mediterranean during the Late Quaternary. *Mar. Micropaleontol.* 2, 353–370.
- Zonneveld, K.A.F., Versteegh, G.J.M., de Lange, G.J., 2001. Paleoproduction and post-depositional organic matter decay reflected by dinoflagellate cyst assemblages of the Eastern Mediterranean S1 sapropel. *Mar. Geol.* 172, 181–195.